Supporting Information

A binuclear zinc complex (Zn_2L) as ratiometric probe for the pyrophosphate (PPi) sensing

Mengxia Liu [a, 1], Wenwen Sun [a, 1], Le Wang [a, *], Zhiqiang Niu [b, *], Xiao Zhang [a], Dingjia Xiao [c], Tianjia Xiao [c], Junfeng Wang [c, *]

[a] College of Chemistry and Chemical Engineering, Shanghai University of Engineering Science, Shanghai 201620, China. E-mail: wangle316@sues.edu.cn

[b] State Key Laboratory of Chemical Engineering, Department of Chemical Engineering, Tsinghua University, Beijing 10084, China. E-mail: niuzq@tsinghua.edu.cn

[c] Gordon Center for Medical Imaging, Massachusetts General Hospital and Harvard Medical School, 125 Nashua Street, Suite 660, Boston, Massachusetts 02114, USA.

E-mail: jwang83@mgh.harvard.edu

[1] These authors contributed equally to this work and should be considered co-first authors.

Table of contents

1. Experimental section

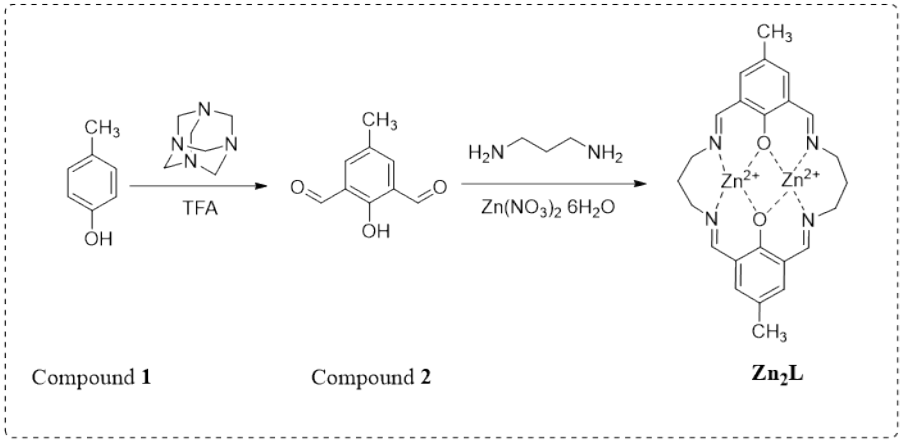

Fig. S1 Synthesis route of probe Zn_2L

Synthesis of the Compound 2: The Compound 2 was synthesized according to the literature and improved [1]. Hexamethylenetetramine (11.2 g, 80 mmol) was dissolved in 15 mL of trifluoroacetic acid (TFA), then 4-methylphenol (2.16 g, 20 mmol) was added and stirred at 105 °C for 12 h. The reaction vessel was then poured with 10 mL of water, and then the reaction solution was refluxed for 10 min, and then slowly added to 400 mL of ice water to quench the reaction. The yellow compound 2 (yield: 82.3%) was obtained by filtration and vacuum drying. ^{1}H NMR (400 MHz, DMSO-d_6) δ 11.40 (s, 1H), 10.21 (s, 2H), 7.85 (s, 2H), 2.33 (s,3H). ^{13}C NMR (101 MHz, DMSO-d_6) δ 192.72, 160.80, 137.80, 129.73, 123.72, 19.99.

Synthesis of the Zn_2L: The binuclear complex Zn_2L was synthesized according to the literature and improved [1]. 1,3-diaminopropane (1 mmol, 84 μL) was added to the methanol solution of Zn $(NO_3)_2$ $6H_2O$ (0.3 g, 1 mmol, 5 mL), and then a methanol solution of Compound 2 (1 mmol, 5 mL) was added. The resulted mixture was stirred under reflux for one hour. Yellow crystals (yield: 85.6%) precipitated after standing for several hours and were collected by filtration. ^{1}H NMR (400 MHz, DMSO-d_6) δ 8.51 (s, 4H), 7.54 (s, 4H), 3.98 (s, 8H), 2.29 (s, 6H), 2.04 (s, 4H). ^{13}C NMR (101 MHz, DMSO-d_6) δ 170.68, 164.82, 142.76, 125.93, 121.24, 62.73, 29.49, 19.72.

2. Characterization of Compound 2 and Zn_2L probe

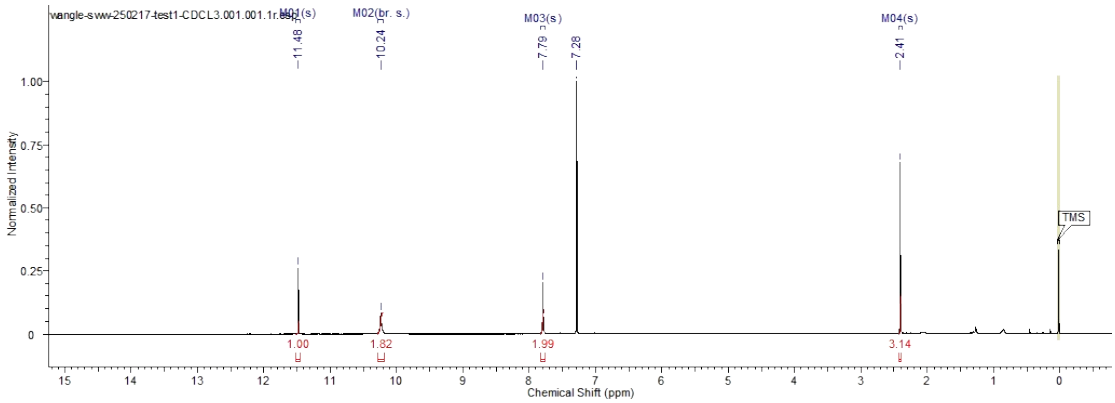

Fig. S2 ^{1}H NMR spectra of Compound 2 in $CDCl_3$.

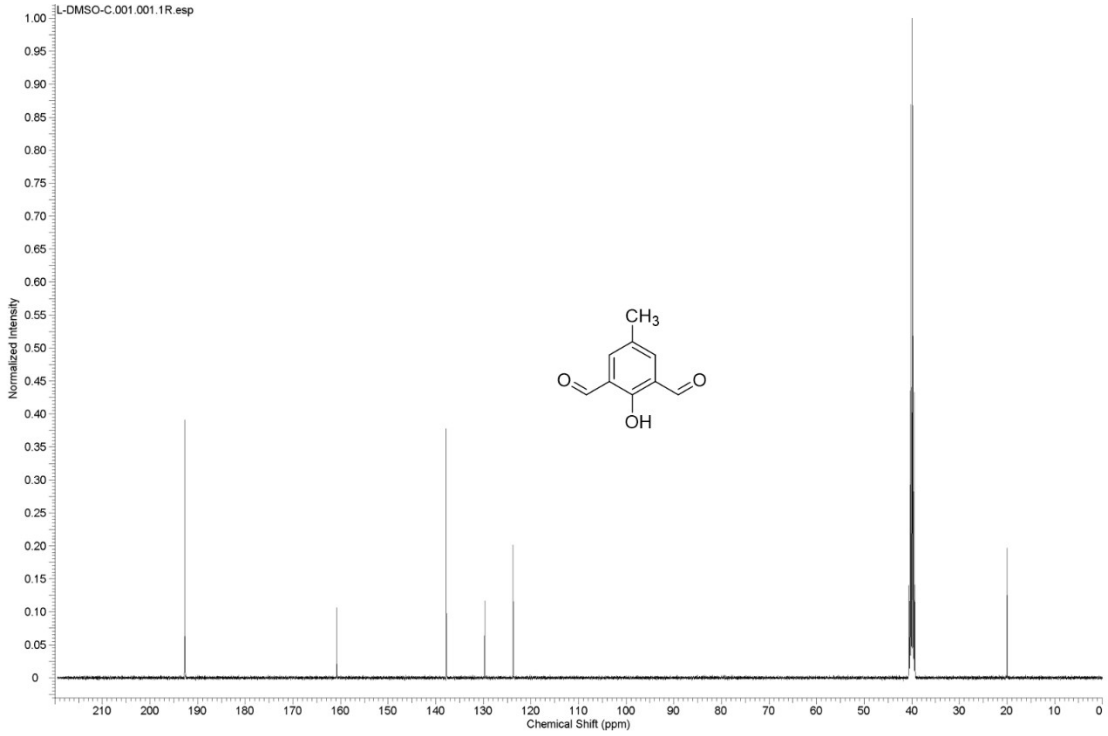

Fig. S3 ^{13}C NMR spectra of Compound 2 in DMSO-d6.

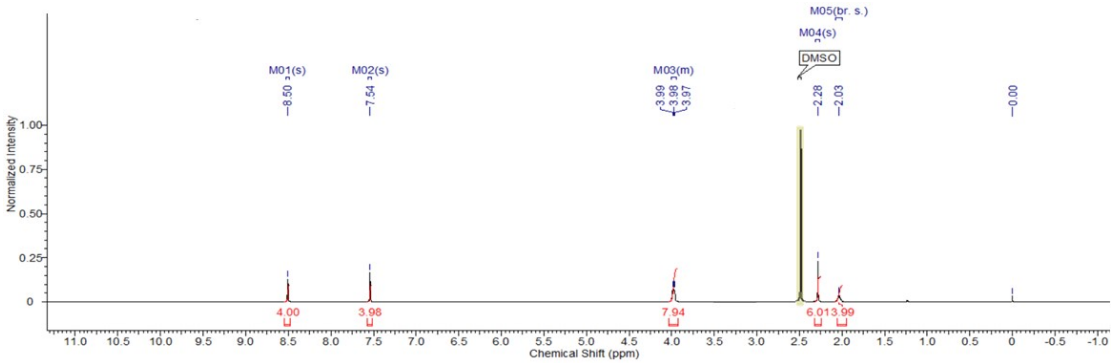

Fig. S4 ^{1}H NMR spectra of Zn_2L in DMSO-d_6.

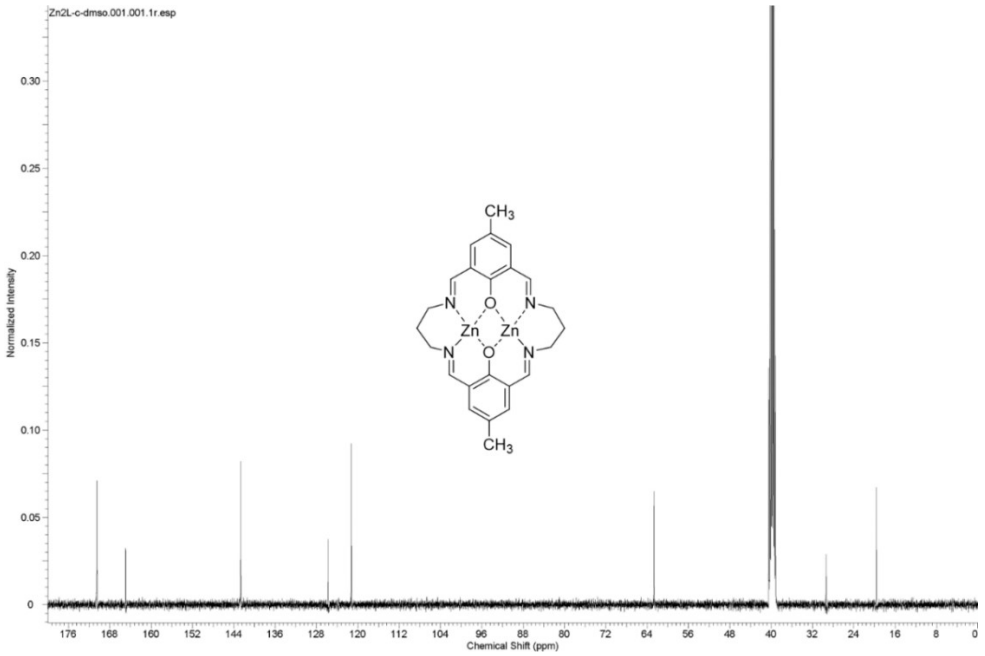

Fig. S5 ^{13}C NMR spectra of Zn_2L in DMSO-d6.

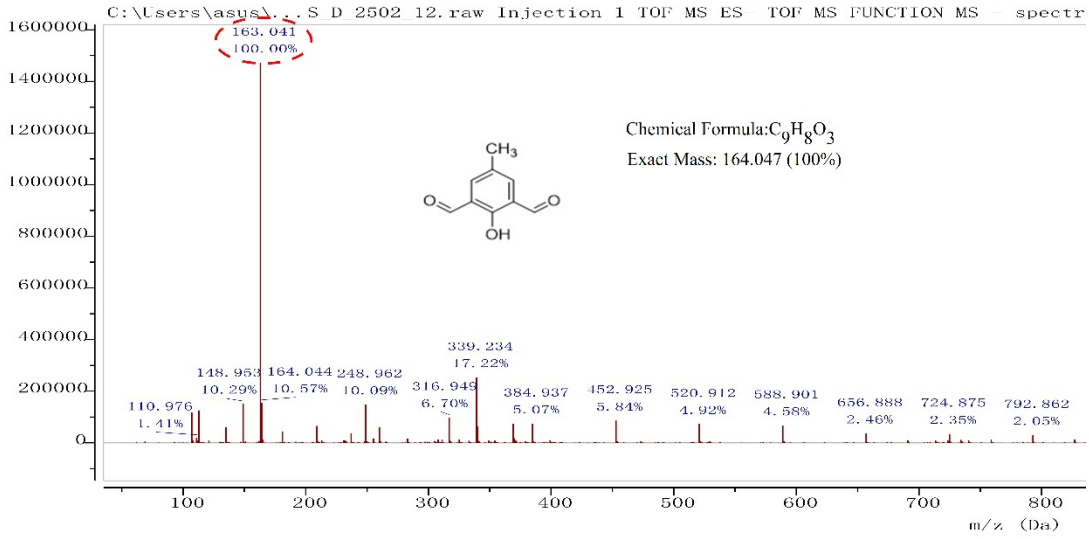

Fig. S6 The mass spectrometry of complex 2 in negative ion mode.

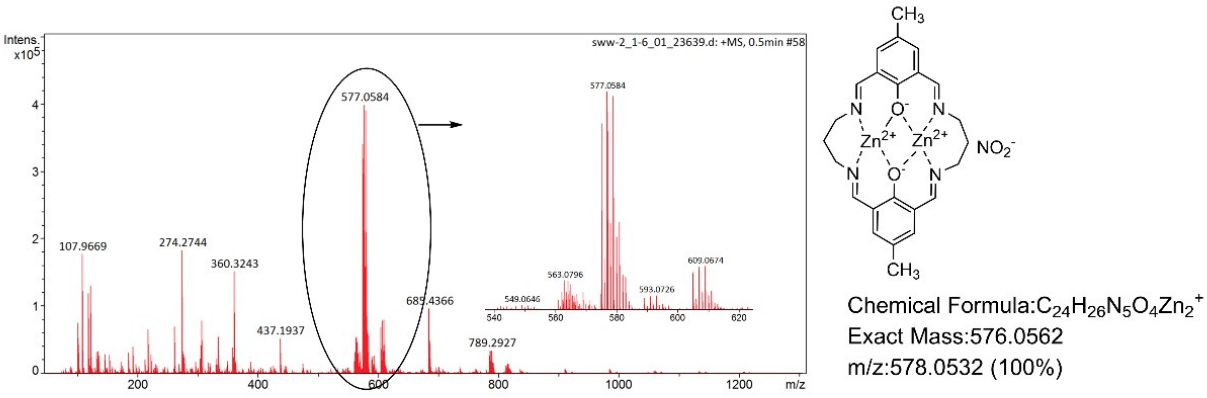

Fig. S7 The mass spectrometry of complex Zn_2L in positive ion mode.

3. Real sample analysis

Urine samples were collected from volunteers from SUES (shanghai university of engineering science). This study strictly adheres to the "Ethical Review Measures for Biomedical Research Involving Humans,"[2] and all participants were fully informed of the research purpose, potential risks, and benefits prior to sample collection.

4. Optimization of experimental conditions

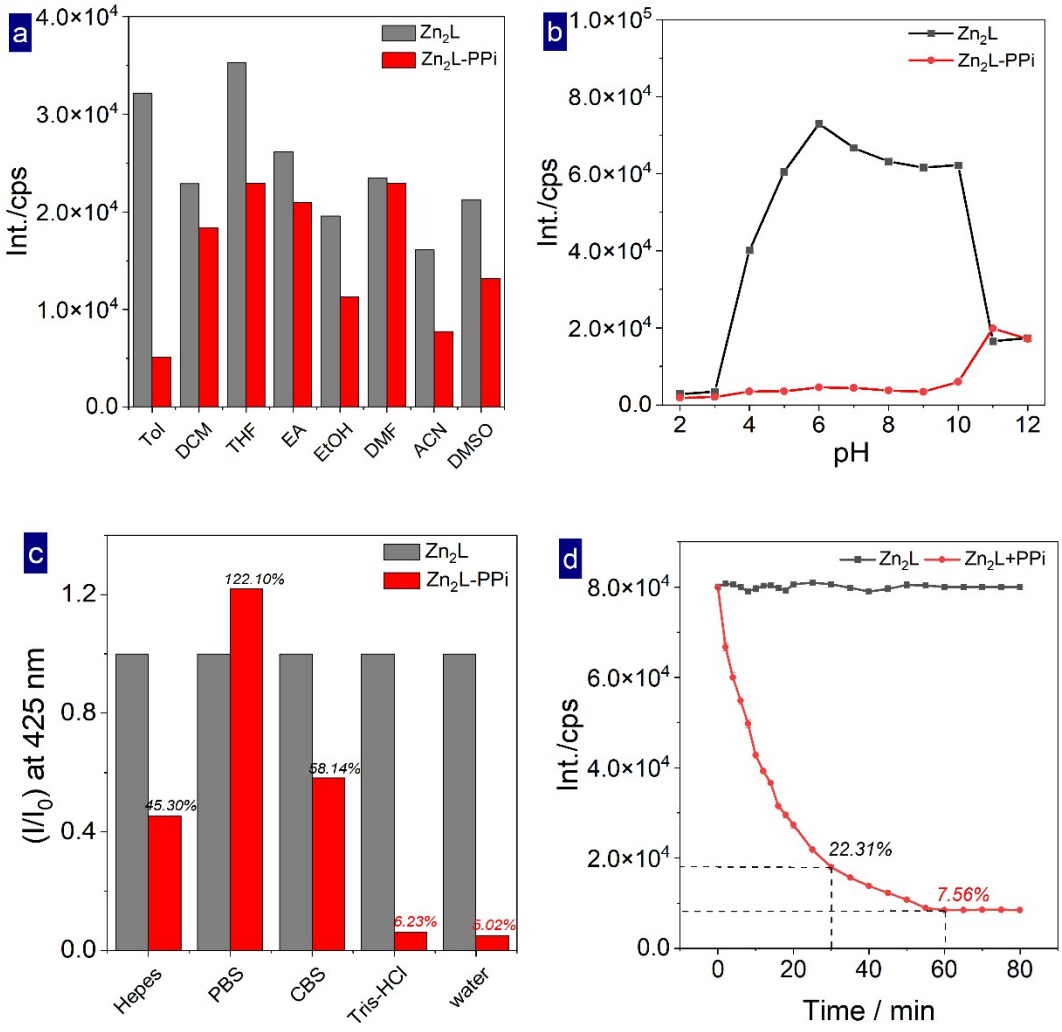

Fig. S8 (a) Histogram of the highest point of fluorescence intensity of the Zn_2L probe (5 μM) for the detection of PPi (50 μM) in different solution systems (Tol: Toluene; DCM: Dichloromethane; THF: Tetrahydrofuran; EA: Ethyl Acetate; EtOH: Ethanol; DMF: N,N Dimethylformamide; ACN: acetonitrile; DMSO: Dimethyl Sulfoxide) at 425 nm; (b) Changes in fluorescence intensity of the probe Zn_2L (10 μM) for recognizing PPi (100 μM) in water solution with different pH conditions; (c) Histogram of the highest point of fluorescence intensity of the Zn_2L probe (10 μM) for the detection of PPi (100 μM) in HEPES (pH=7.0, 10 mM), PBS (pH=7.4, 10 mM), CBS (pH=9.2, 10 mM), Tris-HCl (pH=7.4, 10 mM) and water solution systems at 425 nm; (d) Fluorescence intensity at 425 nm for Zn_2L (10 μM) in the presence of PPi (100 μM) as a time-dependent in Tris-HCl (pH=7.4, 10 mM).

5. Study of binding constants

The K_{b1}= 2.12×10^7 M^{-1} (R^2=0.990) (**Fig. S7a**) for the 1:1 complex and K_{b2}= 2.14×10^{12} M^{-1} (R^2=0.994) (**Fig. S7b**) for 1:2 binding process of the probe to PPi were calculated based on the following equation (1). [3]

$$\log\left[\frac{F-Fmax}{Fmin-F}\right] = logK_b + nlog[S] \quad (1)$$

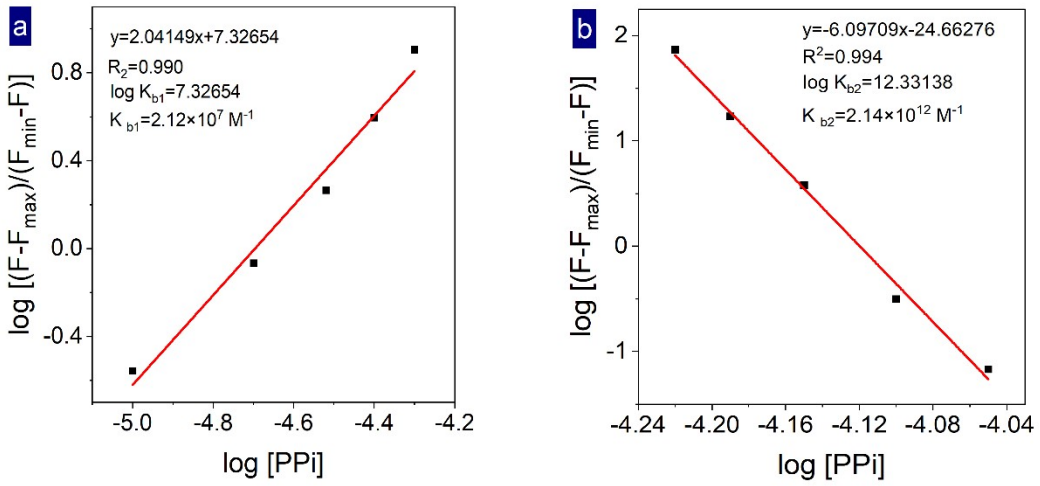

Fig. S9 (a) Binding constant curves for the binding process of Zn_2L to PPi in 1:1 complex; (b) Binding constant curves for the binding process of Zn_2L to PPi in 1:2 complex.

6. The chemical structures of PPi homologous compounds

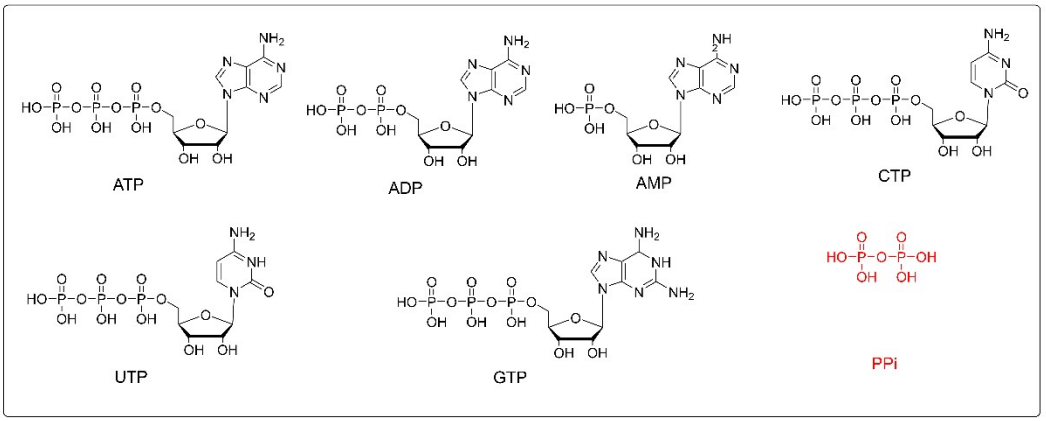

Fig. S10 The chemical structures of PPi homologous compounds (ATP, ADP, AMP, CTP, UTP and GTP).

7. Table

Table S1 Fluorescence quantum yield of probe Zn_2L in different solvents

Solvent	Zn_2L
EA	0.034
THF	0.115
Ethanol	0.038
Methanol	0.028
ACN	0.021
DMF	0.045
DMSO	0.088
H_2O	0.020

*：The fluorescence quantum yield of the probe Zn_2L was obtained by measurement using an ethanol solution of rhodamine B (Φ_R=0.89) as a reference, calculated as follows (2): [4]

$$\Phi_s = \Phi_R(\frac{A_R}{A_S})(\frac{F_S}{F_R})[\frac{n_S}{n_R}]^2 \quad (2)$$

where Φ_S and Φ_R are the fluorescence quantum yields of the probe and rhodamine B, respectively, A_S and A_R are the absorbance of the probe and rhodamine B at the excitation wavelength, F_S and F_R represent the integral areas of the fluorescence emission spectra of the probe and rhodamine B, and n_S and n_R denote the refractive indices of the solvents used for the probe and rhodamine B.

Table S2. Summary of PPi sensors and their structures, fluorescence sensing and applications

No.	Chemical Structures	$\lambda_{ex}/\lambda_{em}$ (nm)	LOD (μM)	Applications（Medium）	Refs
NO.1	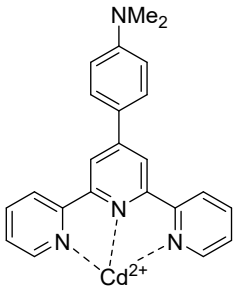	400/580	200	HeLa cell imaging	[5]

NO.2	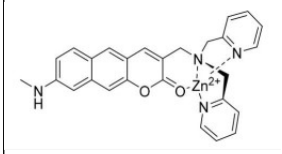	400/595	--	HeLa cell imaging/Locate lysosomes	[6]
NO.3	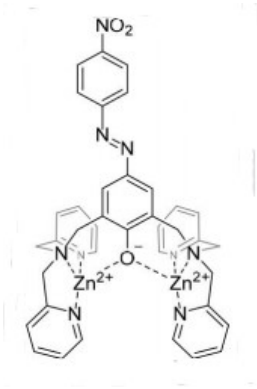	--	--	--	[7]
NO.4	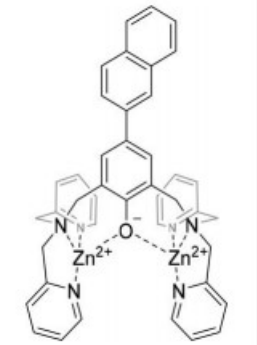	280/316	About μM	--	[8]
NO.5	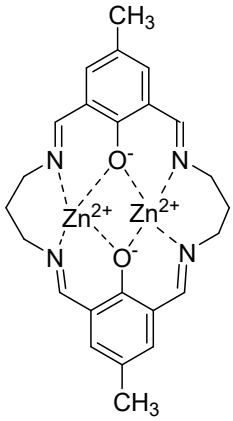	390/500	0.29	PPi sensing/ Detection of PPi in human metabolic urine	This work

8. The experiments of ^{31}P NMR titration

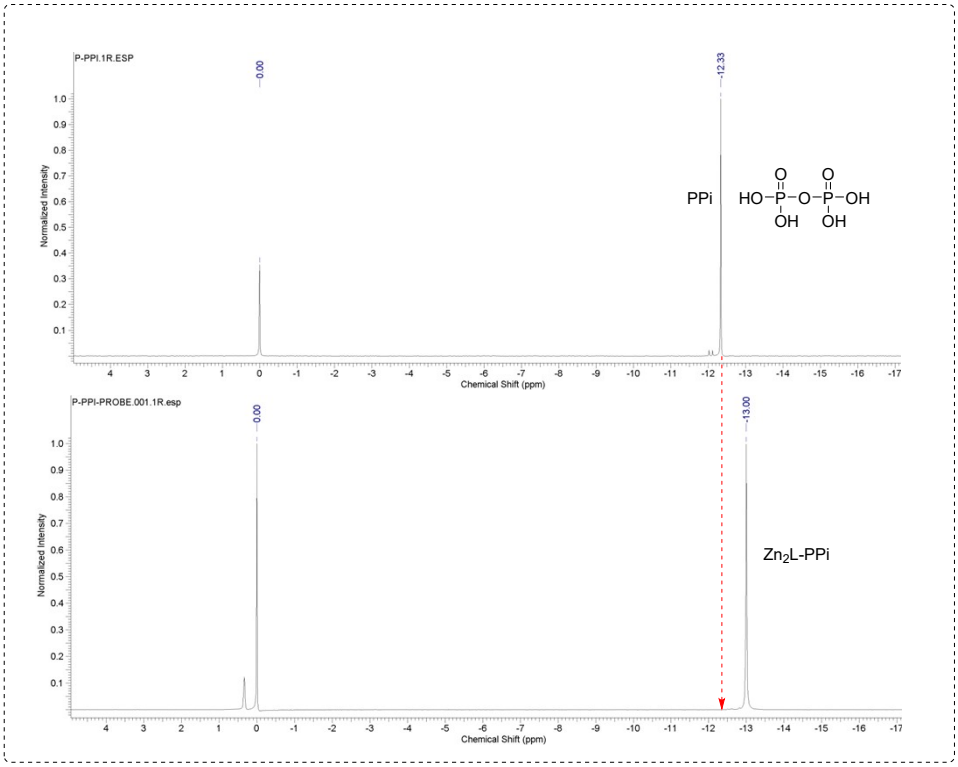

Fig. S11 ^{31}P NMR spectra of PPi and Zn_2L-PPi in DMSO-d_6.

9. Theoretical calculation

Table S3. Vertical excitation of Zn_2L-PPi.

Compound	Electronic transition	Energy, eV	f[a]	Composition[b]	Contribution %
Zn_2L-PPi	$S_0 \rightarrow S_1$	1.10	0.0006	HOMO→LUMO	99.86
	$S_0 \rightarrow S_2$	1.84	0.0012	HOMO→LUMO+1	99.66
	$S_0 \rightarrow S_3$	2.31	0.0115	HOMO→LUMO+2	95.03
	$S_0 \rightarrow S_4$	1.92	0.0001	HOMO-1→LUMO	59.82
	$S_0 \rightarrow S_5$	3.03	0.0000	HOMO-2→LUMO	59.43

10. Photophysical properties of the Compound 2 and Zn_2L response to PPi

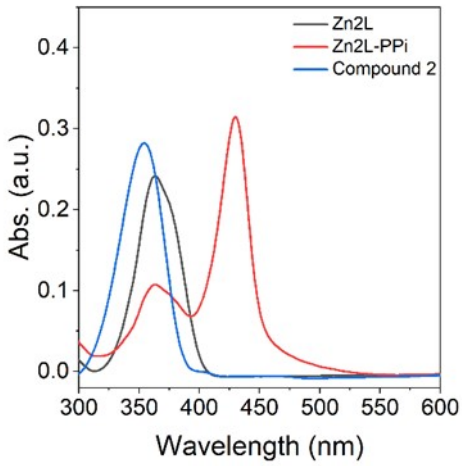

Fig. S12 UV response to Compound 2, Zn_2L (10 μM) and PPi (100 μM) in Tris-HCl (pH=7.4, 10 mM).

11. References

[1] Zhang, S.; Xue, Y.; Wu, Y.; Zhang, Y. X.; Tan, T.; Niu, Z., PET recycling under mild conditions via substituent-modulated intramolecular hydrolysis. *Chemical science* **2023**, 14, (24), 6558-6563. https://doi.org/10.1039/d3sc01161e.

[2] Li B. Ethical Review Measures for Biomedical Research Involving Humans. 2022.

[3] Cao H, Wu D, Wang H, Xu M. Effect of the glycosylation of flavonoids on interaction with protein. Spectrochim Acta A. 2009;73(5):972-975. https://doi.org/10.1016/j.saa.2009.05.004.

[4] Tang L, Mo S, Liu SG, Liao LL, Li NB, Luo HQ. Synthesis of fluorescent polydopamine nanoparticles by Michael addition reaction as an analysis platform to detect iron ions and pyrophosphate efficiently and construction of an IMPLICATION logic gate. Sens. Actuators B Chem. 2018;255:754-762. https://doi.org/10.1016/j.snb.2017.08.069.

[5] Purohit, A. K.; Ghosh, B. N.; Kar, P. K., Selective detection of pyrophosphate anion by a simple Cd (II) based terpyridine complex. *Spectrochimica acta. Part A, Molecular and biomolecular spectroscopy* **2018**, 188, 547-550. https://doi.org/10.1016/j.saa.2017.07.048.

[6] Tamima, U.; Sarkar, S.; Islam, M. R.; Shil, A.; Kim, K.\H.; Reo, Y. J.; Jun, Y. W.; Banna, H.; Lee, S.; Ahn, K. H., A small‐molecule fluorescence probe for nuclear ATP. *Angewandte Chemie International Edition* **2023**, 62(15), 2-8. https://doi.org/10.1002/anie.202300580.

[7] Lee, D. H.; Im, J. H.; Son, S. U.; Chung, Y. K; Hong, J. I., An azophenol-based chromogenic pyrophosphate sensor in water. *Journal of the American Chemical Society* **2003**, 125(26), 7752-7753.

[8] Lee, D. H.; Kim, S. Y.; Hong, J. I., A fluorescent pyrophosphate sensor with high selectivity over ATP in water. *Angewandte Chemie* **2004**, 43, (36), 4777-4780. https://doi.org/10.1002/anie.200453914.